Available online at www.sciencedirect.com
ScienceDirect
Atmospheric Environment 42 (2008) 3571–3583
ATMOSPHERIC ENVIRONMENT
www.elsevier.com/locate/atmosenv

MICS-Asia II: Modeling gaseous pollutants and evaluating an advanced modeling system over East Asia

Joshua S. Fu[a,*], Carey J. Jang[b], David G. Streets[c], Zuopan Li[a], Roger Kwok[a,d], Rokjin Park[e,f], Zhiwei Han[g]

[a]*Department of Civil and Environmental Engineering, The University of Tennessee, Knoxville, TN 37996, USA*
[b]*Office of Air Quality Planning and Standards, US Environmental Protection Agency, 109 T.W. Alexander drive, RTP, NC 27711, USA*
[c]*Argonne National Laboratory, 9700 South Cass Avenue, Argonne, IL 60439, USA*
[d]*Department of Mathematics, Hong Kong University of Science and Technology, Clear Water Bay, Kowloon, Hong Kong*
[e]*Division of Engineering and Applied Science, Harvard University, 29 Oxford Street, Cambridge, MA 02138, USA*
[f]*School of Earth and Environmental Sciences, Seoul National University, San 56-1, Sillim, Gwanakgu, Seoul 151-742, South Korea*
[g]*Institute of Atmospheric Physics, Chinese Academy of Sciences, 100029 Beijing, China*

Received 2 March 2007; received in revised form 24 July 2007; accepted 30 July 2007

Abstract

An advanced modeling system with a "one-atmosphere" perspective, Models-3/Community Multi-scale Air Quality (CMAQ) modeling system, driven by MM5/NCEP reanalysis data as the meteorology, and GEOS-Chem outputs as boundary values was applied to simulate the O_3, and other gaseous pollutants (SO_2 and NO_2) evolution among other atmospheric chemicals for July 2001. Comparisons had been made with other models in the MICS-II exercise for the same period. Statistics of both monthly and daily means show that the model skill is very good in reproducing O_3 and SO_2 with small to moderate RMSE. The model species capture the day-to-day and spatial variability of the observations. The same O_3 model concentrations that overpredict most of the EANET observations in the MICS-II study may have underpredicted ones from monitoring networks in Beijing area that is not included in this paper. Vertical O_3 profiles at 4 ozonesonde sites are well predicted in July 2001. In fact, our model is among the best of those MICS-II models within the 2-km surface layer. The meteorology near surface and lower troposphere is well reproduced. Compared to SO_2 and O_3, the NO_2 gas concentrations are simulated less well, but the correlation coefficient is still significant.

The choice of reanalysis meteorological fields and different boundary conditions generated by different global models may result in diverse spatial patterns exhibited by MICS-II models and ours. Our spatial distributions of O_3 shows a high concentration patch covering Beijing, a moderate to high pattern across Korea and Japan Sea, and a low but extensive pattern enclosing southern China, Taiwan, and East Sea. Extension of the pattern to southern China coincides with the existence of pollution problems in Guangdong and Taiwan, but overprediction of O_3 over the region deserves further improvement by various factors. One of them can be the grid resolution to resolve the complex orography in or close to the ocean. Another factor can be the refinement of local land use data that changes the micro-meteorology in favor of more air pollution events. Published by Elsevier Ltd.

Keywords: CMAQ; EANET; GEOS-Chem; Model performance; TRACE-P

*Corresponding author. Tel.: +1 865 974 2629; fax: +1 865 974 2669.
E-mail address: jsfu@utk.edu (J.S. Fu).

1352-2310/$ - see front matter Published by Elsevier Ltd.
doi:10.1016/j.atmosenv.2007.07.058

1. Introduction

Air pollution is damaging public health, air and water quality, agriculture, industry, and it will deteriorate the economy and health conditions. In order to realize its sustainable development of energy and maintain its public health, countries must control their air quality, study the health impact of air pollutants, and grasp the ability to study and forecast air pollutant parameters. Effective energy and environmental policies can play active roles for the future air quality and public health improvements by legislatorial and regulatory controls over energy consumption and air pollutant emissions, while modeling and simulation studies can provide opportunities to look into the future environmental situation and provide helpful information for the government to take legal steps for better air quality controls and better public health. The rate of success to prevent avoidable health disaster can be enhanced by close collaboration between public health and energy policy with the help of modeling studies. East Asia is the world's most populous region with a fast growing economy that surges in energy consumption. It includes China that has become the second largest energy consumer after the United States although the per capita level is much lower than those found in developed or developing countries (Streets et al., 2003). More coal is burnt in power plants and more fuel is used in industrial boilers and furnaces to meet the development of economy. The energy demand snows and more fuel is consumed in the upsoaring number of cars. The impact of economy growth on the air quality is so severe that concentrations of most pollutants remain high in most industrial and metropolitan regions. Using an air quality model to assess the impacts of air quality from those gaseous pollutants is critical for atmospheric chemistry studies and for the development of environmental management strategies (National Research Council (NRC), 1991) and plays a role for the decision makers. Air quality models are usually used to quantify pollutants in the atmosphere. A number of air quality models have been developed and employed in many problems. For instance, Regional Air Quality Model (RAQM) (An et al., 2002; Han et al., 2006a), ATMOS long-range transport model (Arndt et al., 1998), and Air Quality Prediction Modeling System (AQPMS, Wang et al., 2002) were applied to study precipitation pollutants; Regional Acid Deposition Model (RADM) with CIT gas chemistry and aerosol process (Chang and Park, 2004) for dust events; Regional Atmospheric Modeling System (RAMS, Hayami and Ichikawa, 2001) for sulfur transport; a Lagrangian puff model ATMOS-N (Holloway et al., 2002) to calculate source–receptor relationships for reactive nitrogen species in Asia; and CTMs to model gaseous and aerosol pollutants in support of the TRACE-P experiment (Carmichael et al., 2003; Kiley et al., 2003). Sole modeling of atmospheric chemistry includes works on photochemical model intercomparison (Olson et al., 1997) and on gas–aerosol equilibrium to the moisture and species in aerosols observed in central Japan (Ueda et al., 2000). Other applications focus on natural emission sources, such as massive SO_2 released by volcanic eruptions using a regional-scale Eulerian Model System for Soluble Particles (MSSP, Kajino et al., 2004) and the impact of biogenic emission on regional ozone using TCTM with MM5 (Han et al., 2005). Intercomparison among models takes in many forms. The most common one is Eulerian to Eulerian on global transport of carbon monoxide (Kanakidou et al., 1999), on ^{222}Rn as a tracer (Jacob et al., 1997), and a rather recent one on sulfur depositions (Carmichael et al., 2002). Another kind of comparison is Lagrangian–Eulerian on sulfur deposition in East Asia (Phadnis et al., 1998).

The purposes of the paper are to evaluate the performance of Models-3/CMAQ model in simulating ozone and relevant gaseous chemical species in the study of East Asia region, and to compare the consistency and discrepancy with observation data collected by a wide monitoring network, Acid Deposition Monitoring Network in East Asia (EANET), Japan Meteorological Agency (JMA). A model intercomparison study—MICS-Asia, Phase II—examined in March, July, and December 2001, and in March 2002. An additional feature unique to Phase II is the inclusion of global inflow to the study domain with new observational data obtained under the EANET (the Acid Deposition Monitoring Network in East Asia) monitoring program, were made available for this study, and these data provided a region-wide data base to use in the comparisons. Nine modeling groups using three-dimensional Eulerian models were analyzed in MICS-II, including a model from Korea; the PATH model; the RAQM model; the MSSP model; the STEM model; the MATCH model; the Polair3D model; and two applications of the CMAQ model (http://www.epa.gov/asmdnerl/CMAQ/). In this paper the abilities to predict ozone and other gaseous

pollutants in East Asia of 8 MICS-II models have been evaluated (Carmichael et al., 2008). The considered species in this paper include SO_2, NO_2, and O_3. The analysis follows the MICS-II work based on the relative completeness of observation data and their significance in atmospheric chemistry and climate change. The paper provides the Models-3/CMAQ to conduct the model assessment and to evaluate ozone and relative pollutants in East Asia region. It illustrates the abilities of the model in the degree of agreement and limitations of regional assessment as well as provides valuable information and implications for further model improvement.

2. USEPA's Models-3/CMAQ modeling system

Over a decade, USEPA devoted major resources for developing an advanced modeling system with a "one-atmosphere" perspective, i.e., the USEPA's Models-3/Community Multi-scale Air Quality (CMAQ) modeling system (Byun and Ching, 1999; Byun and Schere, 2006). Models-3/CMAQ is a numerical modeling system that can simultaneously simulate the transport, physical transformation, and chemical reactions of multiple pollutants across large geographic regions. The system is useful to states, other governments and international agencies for making regulatory decisions on air quality management, as well as to research scientists for performing atmospheric research. It is a combination of Models-3, a flexible software framework, and the CMAQ modeling system for supporting air quality applications ranging from regulatory issues to scientific research on atmospheric processes. A modular science design of CMAQ allows the user to build different chemistry-transport models for various air quality problems. The "one-atmosphere" Models-3/CMAQ system was designed to approach air quality as a whole by including state-of-the-science capabilities for modeling multiple air quality issues, including ozone, particulate matter, visibility degradation, acid deposition, and air toxics, at multiple scales. The Models-3/CMAQ system was first released to the public in July 1998 and had a recent update release in October 2005.

3. Model configuration and setup

3.1. Model domain

In this Models-3/CMAQ application, the model domain covered the Great China region and in Fig. 1, 36 km × 36 km grid resolutions set up by the MM5 meteorological processing model for July in 2001 used in USEPA's Regional Air Quality Modeling (Streets et al., 2007) in the East Asia in this study. The domains had 164 × 97 horizontal grid cells using a 36-km resolution based on Lambert Conformal map projection centered at (34°N, 102°E). Fourteen vertical layers were configured initially following the sigma (σ) layer structure with denser grids at lower levels to better resolve the boundary layer. The σ-layer interfaces occurred at: 1 (0), 0.995 (38 m), 0.988 (92 m), 0.98 (153 m), 0.97 (230 m), 0.956 (340), 0.938 (482 m), 0.893 (846 m), 0.839 (1300 m), 0.777 (1850 m), 0.702 (2557 m), 0.582 (3806 m), 0.400 (6083 m), 0.20 (9511 m), and 0.00 (16,262 m).

3.2. Model configuration

The October 2004 release version of Models-3/CMAQ (version 4.4) system was used in this modeling work. Further details of model configuration and science modules are given in Models-3/CMAQ science document (Byun and Ching, 1999; Byun and Schere, 2006) and recent release note in 2004. The key science modules used in this modeling work are given below. Note that the selected science modules are the default options given in the October 2004 Models-3/CMAQ release version.

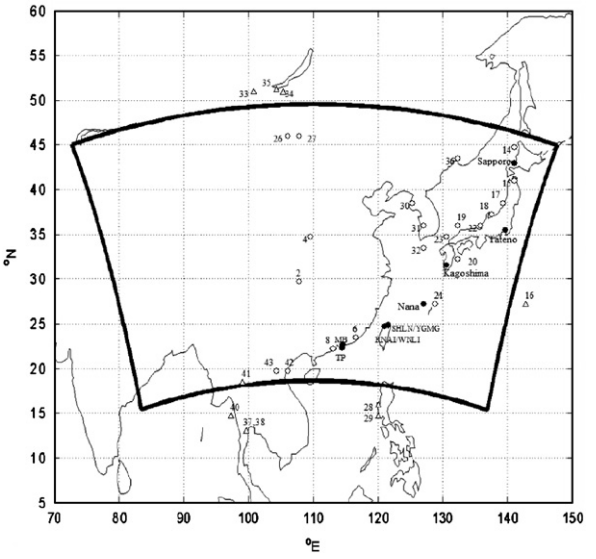

Fig. 1. CMAQ modeling domain and locations of ground-level monitoring sites of EANET (open circle denotes sites within the common domain, open triangle presents sites outside of the domain, and closed circle is the locations of O_3 sounding sites, ID numbers of each site are also shown).

The background initial and boundary conditions for the 36-km domain are based on nesting from global chemical transport model, GEOS-Chem, results (Heald et al., 2003) to wash out the first 5 days during the model runs.

3.3. Model inputs and setup

The Mesoscale Model Version 5 (MM5) v3.6 was used to provide meteorological input fields for the model simulations. The 36-km domain and its meteorological outputs simulated by MM5 in the USEPA's Great Asia modeling effort (Streets et al., 2007) were used in this work. The newest Meteorology/chemistry Interface Processor (MCIP) 2.2 that corrected layers collapsing released in June 2003 was used to process the raw MM5 output data into the format and structure required by the Models-3/CMAQ modeling. The configuration specifications can be referred to in Table 1.

3.4. Emission estimates

Inventories of 11 major chemical species have been developed by the TRACE-P project (Streets et al., 2003), including SO_2, NO_x, CO_2, CO, CH_4, non-methane volatile organic compounds (NMVOC), black carbon aerosol (BC), organic carbon aerosol (OC), NH_3, PM_{10}, and $PM_{2.5}$. Detailed emissions are considered by type of fossil fuel for the sectors of anthropogenic combustion, which are aggregated into five primary source categories of industry, residential, transportation, power generation, and agriculture. Biomass burning is calculated independently in three major categories: forest burning, savanna/grassland burning, and the burning of crop residues. Emission inventories are updated to year 2000 for each country in Asia and for each province of China. Annual total emissions of 11 pollutants with 18 subcategories of NMVOC are developed by the TRACE-P project. This is not directly compatible with the needs of Models3-CMAQ, which requires the Carbon Bond IV Chemical Mechanism (CB-4) as 22 species. Different species of NMVOC will be merged into higher aldehyde based acetaldehyde (ALD2), ethane (ETH), formaldehyde (FORM), olefin carbon bond (OLE), paraffin carbon bond (PAR), toluene and other monoalkyl aromatics (TOL), and xylene and other polyalkyl aromatics (XYL); $PM_{2.5}$ and PM_{10} will be divided into fine aerosols in light of the speciation profile developed by USEPA [used by the sparse matrix operator kernal emission (SMOKE) model (Carolina Environmental Programs, 2003) as files the chemical speciation profiles (GSPRO) and speciation cross-reference (GSREF)]; and biogenic isoprene (ISOP) and terpenes (TERPB) will be directly prepared by GIS based on land-use information. Only domestic, agriculture, biomass burning, and biogenic sectors are assumed to have seasonal variation in China in the TRACE-P project. Monthly operation hours of stoves for domestic heating will be estimated based on monthly mean temperatures for each province in China. Combustion emissions for the domestic sector in January and July will be estimated based on the monthly profiles of stove hours. The weekly and hourly profiles have been developed.

Table 1
Basic structures, schemes, and relevant parameters of the CMAQ model

Models	CMAQ
Domain	15.4°N–49.5°N 72.7°E–147.7°E
Horizontal resolution	36 km
Vertical resolution	14 σ_p levels
Depth of 1st layer	38 m
Model top	16 km
Projection	Lambert
Meteorology	MM5/NCEP
Advection	Piecewise parabolic
Vertical diffusion	K-theory
Dry deposition	Wesely (1989)
Wet scavenging	Henry's Law
Gas chemistry	CB-IV
Aqueous chemistry	Walcek and Taylor (1986)

Lambert: the Lambert projection is the one of the most commonly used map projections and the only commonly used conic projection that displays the poles as points they truly are. Piecewise parabolic: for gas dynamics in Lagrangian and Eulerian coordinates (Collela and Woodward, 1984).

4. Results and discussions

4.1. Monthly mean concentrations

4.1.1. Statistics of modeled and ground level observations of SO_2, NO_2, and O_3

Table 2 shows the statistics for the monthly mean concentrations of SO_2, NO_2, and O_3 for the case of July 2001 only. Although the sample sizes are relatively small (15 for SO_2, 13 for NO_2, 10 for O_3), the correlation coefficients are high compared with

other models in the MICS-Asia II study (Carmichael et al., 2008), suggesting the satisfactory matching between the model results and the site observations.

The model captures SO_2 very well with correlation 0.726. Further, while most MICS-II models exhibit positive mean bias errors (MBE), it has small negative MBE, implying slight underprediction. The root mean square error (RMSE) is also in a lower range among those models.

O_3 is also well modeled, with correlation 0.725, MBE 6.75 ppb and RMSE 10.3 ppb. The errors are moderate among all the other models. While the model overpredicts the O_3 with respect to the EANET site observations, it is possible that the same model may have underpredicted the reality. According to personal communications, observation data collected by Zhang, Y. at Peking University generally exhibit higher concentrations over the Beijing–Tianjin regions (Fig. 1 in Streets et al., 2007).

Compared to SO_2 and O_3, the NO_2 gas concentrations are simulated less well. The MBE and RMSE are quite low, implying that there is a small difference in magnitude, and that the underprediction is minor. Note the negative MBE in NO_2 corresponds to the positive MBE in O_3, suggesting accumulation of O_3 in less NO_x available for titration.

4.1.2. *Modeled and observed monthly SO_2, NO_2, and O_3 means at EANET sites July 2001*

Fig. 2 displays the modeled and observed ground level monthly mean concentrations of SO_2, NO_2, and O_3 for July 2001. Note the logarithmic scales in SO_2 and NO_2, and the linear scale in O_3. Despite the relatively small sample sizes, our model (in bright green circle) performs well in capturing the overall spatial distribution as well as the magnitudes at most of the EANET sites.

For SO_2, the least deviation from the observations occurs at sites 2, 4, 8, and 23. The most noticeable deviation occurs at site 6 where the observations are underpredicted significantly. Sites 2, 4, 8, and 6 come from Jinyunshan, Weishuiyuan, Xiangzhou, and Hongwen, China, respectively. Three out of the four give rise to satisfactory SO_2 prediction, suggesting that the SO_2 emissions in China are already well allocated at accurate enough position and at about the right amount.

NO_2 sites 2, 8, 15, 17, 19, and 23 are well modeled, while the worst occurs at site 16: the model concentration is certainly out of range, presumably underpredicting the observations there. Among the well modeled are also in Jinyunshan and Xiangzhou, China. The location of site 16 where the worst model result occurs is Ogasawara, Japan, possibly for the same reason of poor performance of most of the other models: Ogasawara is further downwind of the Asian continent so that the model meteorology may have diluted model NO_2 along the air passage to the place.

Our model displays much less O_3 deviation across available sites than that of NO_2 and SO_2. In fact, it is already capable of capturing the spatial patterns of the observations just like all the other models. Sites 14 and 15 are probably the best to match the observations, while overprediction occurs in other sites except site 18. Overprediction is most eminent at site 16 (Ogasawara), followed by site 21 (Hedo), while the most significant underprediction occurs at site 18 (Tappi). Interesting enough, the well overprediction of O_3 in Ogasawara coincides with the well underprediction of NO_2 at the same place, suggesting that too low NO_2 model concentrations allow for accumulation of the O_3 model concentrations. In contrast, the O_3 underprediction at Tappi by $\sim$10 ppb echoes the NO_2 overprediction by $\sim$6 ppb at the same place: excessive model NO_2 may have titrated with the modeled O_3. In terms of magnitude, error is around 10 ppb as shown in Table 2, and the extreme only go less than 30 ppb.

Table 2
Statistics regarding monthly mean concentrations in July 2001

	R	MBE	RMSE	Sites (pair of sample)
SO_2	0.726	−0.373	2.222	15
NO_2	0.425	−1.004	2.994	13
O_3	0.725	6.750	10.290	10

Comparison for monthly means in July 2001 (unit: ppbv).

4.2. *Daily mean concentrations*

4.2.1. *Comparison with ground level observations of SO_2, NO_2, and O_3*

Table 3 displays the statistics regarding the ground level daily mean concentrations of the modeled and observed SO_2, NO_2, and O_3. The larger sample sizes for the daily mean (SO_2 263, NO_2 225, O_3 153) compared to those for monthly mean (SO_2 15, NO_2 13, O_3 10) should give more credentials to the interpretation of these results.

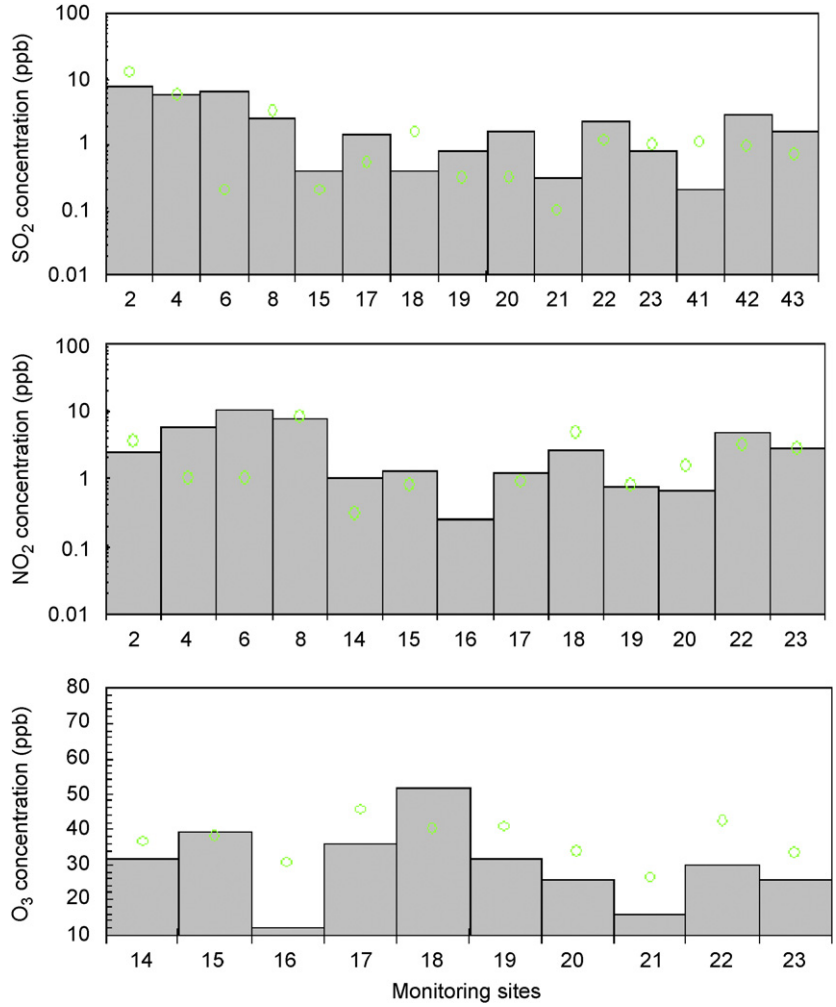

Fig. 2. Comparison of model-derived and observed monthly mean concentrations of SO_2, NO_2, and O_3 at EANET sites in July 2001 (green open circle denotes model results, gray bar means observations).

Here, the O_3 still gives rise to the best prediction compared to the other two gaseous species, with correlation of about 0.72, just the third place to M-7 (0.85) and M-8 (0.79, Carmichael et al., 2008). Although MBE and RMSE are not the least among all the other MICS-II models, they display similar orders of magnitude as for the monthly means. Again, even though the daily means of the model overpredict the EANET observations, the very same model results may have underpredicted observations in Beijing.

SO_2 is also quite well predicted. Correlation is 0.423 which is quite good. The MBE is the lowest in absolute values among all the other models. Only slight negative bias occurs. RMSE is also lower than the other models except M1 and M3. Though correlation is lower than for the monthly mean, the overall statistics is consistent with it. Thus the model is able to reproduce spatial variability as well as the variability in different temporal resolutions of SO_2 in this case.

Table 3
Statistics regarding daily mean concentrations with respect to EANET sites

	R	MBE	RMSE	(Pair of sample)
SO_2	0.423	−0.149	5.069	263
NO_2	0.024	−1.584	4.402	225
O_3	0.717	5.794	13.341	153

Comparison for daily means in July 2001 (unit: ppbv).

NO_2, by contrast, exhibits much less correlation between the model and the observations, although the statistical errors are small. While it has the least correlation in absolute sense among all the other models, the poor model performance in NO_2 is rather universal across them, apparently due to a common input that gives rise to the model outputs. For instance, there could be uncertainties in nitrogen emissions.

4.2.2. Modeled and observed daily O_3 concentrations at Sado site, July 2001

Fig. 3 shows the time series of daily mean O_3 concentrations from our model and from observations at Sado site in July 2001. Complementary to the statistical descriptions in Table 3, the model time series (green bright solid line) in the figure captures the overall trend of the observations. It also picks up the 80 ppb peak on July 10 closer than any other MICS-II models. Ability to capture O_3 peaks is important because without that, it is difficult to pinpoint which emitting species to be reduced so that a control strategy can be carried out effectively. The dip after the July 10 episode is also followed closely by our model up to around July 15, and from July 28 towards the end of the month. During the July 8–15 period, the formation of the O_3 peak is more likely caused by regional transport or local production by VOCs imported from the Asian continent. In either possibility the mesoscale meteorology definitely plays the essential part. In general, the model trend is in phase with the observations throughout the month.

Also note that as for the monthly mean statistics, the daily mean statistics reveal the coincidence of the positive O_3 bias and the negative NO_2, suggesting the likeliness of NO–O_3 titration.

4.3. Vertical profile of O_3 in the western pacific Rim

4.3.1. Comparison of model simulation with O_3 sounding at four aerological stations

There are four aerological stations at Sapporo, Tateno, Kagoshima, and Naha in eastern Asia (Carmichael et al., 2008). Table 4 shows the statistics for the O_3 profiles over certain altitude ranges during July 2001. Our profiles and observations were interpolated into prescribed levels at 50 m increments up to 10 km. The statistics were calculated above and below 5.5 km.

The all high correlation coefficients suggest that our model skill is rather independent of altitude ranges. Even the correlation over all altitudes exceeds 0.7. MBE are small in magnitude except beyond 5.5 km, and mostly negative except within the boundary layer (BL). RMSE are of comparable size within 5.5 km layer, but noticeably larger beyond.

Table 4
Statistics for O_3 profiles derived by comparing with O_3 sounding data at 4 sites in Japan in July 2001 (unit: ppbv)

	R	MBE	RMSE
All altitudes	0.72	−7.10	19.27
<5.5 km	0.77	−1.30	14.48
<2 km	0.73	2.54	17.17
2–5.5 km	0.82	−3.50	12.68
>5.5 km	0.68	−19.98	27.03

In total, 14 observed profiles at 06:00 UTC are used for comparison.

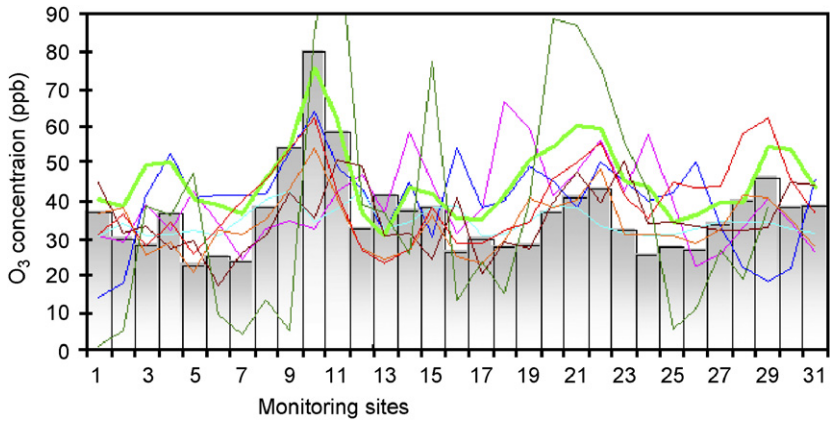

Fig. 3. Time series of model-derived and observed O_3 daily mean concentration at Sado site in July 2001 (bright coarser green line).

Below 5.5 km the correlation is 0.77 with MBE of −1.3. If one further breaks down the altitude range into two layers: namely the BL and the layer range 2–5.5 km, we see lower correlation of 0.73 occurring in the former, and a higher 0.82 in the latter. The respective MBEs show overprediction by 2.5 ppb in BL and underprediction by 3.5 ppb in the 2–5.5 km layer. The RMSE in BL is larger than that in the 2–5.5 km layer. It seems that micrometeorology near the surface imposes some uncertainties that would affect the ground-level concentration, and that the relatively free tropospheric air in the intermediate layer is easier to model, giving rise to a better model–observation agreement.

Beyond 5.5 km, though still high, the correlation diminishes quite noticeably. The MBE is negatively large, not to mention the associated RMSE. The under prediction will be looked in-depth in the next subsection.

Despite the better daily mean statistics of M-7 in July 2001 (see Table 3 here and in Carmichael et al., 2008), our model profile outperforms it as well as all the others within the 2-km BL, and is as good as M-6. It is also worth mentioning that M-7 is also a CMAQ CTM model with similar configuration as ours (see Table 1 here and in Han et al., 2007). The vertical structures differ considerably in configuration at the 16-km altitude for M-7's model top, compared to ours. Thus the associated vertical structures differ substantially. The next noticeable difference is the choice of analysis of meteorological datasets. Spatial distributions of model O_3 will demonstrate the difference later. Therefore our model is capable of capturing the temporal and three dimensional spatial variability at least for the four Japanese ozonesonde sites over the western Pacific Rim.

4.3.2. *Vertical distribution of modeled and observed O_3 at four sites, July 2001*

The model and observed O_3 profiles in July 2001 at Sapporo, Tateno, Kagoshima, and Naha are shown in Fig. 4.

At all stations the model underpredicts the upper tropospheric ozone, from a few ppb to almost 40 ppb. This underprediction is common to all the other models. Although the reason is unclear, possibilities include the uncertainty in prescription of top-layer boundary conditions, and also the limitation of regional models in well representing the upper tropospheric and stratospheric ozone.

The model profile at Sapporo (the location in Fig. 1) follows fairly closely the ozonesonde, though it overpredicts the concentrations within 1 km. In the 1–2 km layer the best model–observation agreement takes place.

At Tateno, surface prediction is very good, with the difference of about 2 ppb. The sharp bend of the ozonesonde around 1 km level denotes an inversion within this layer, where air is stagnant within the layer and therefore pollutants like ozone are trapped. The model can reproduce this feature well, especially the decreasing concentration immediately above the inversion layer. Also note that the surface concentration level is the highest among all the ozonesonde sites. Occurrence of inversion layer is often associated with this concentration level. The model profile stays constant around 40 ppb beyond 3 km while the ozonesonde picks up the increasing trend as altitude increases.

Kagoshima is the best among the 4 sites. The minute difference, only 1 ppb at the surface, carries through up to around 4 km. The diversion from the ozonesonde is not too far compared to the ones in Tateno and Naha, even above the 4 km height. The constant profiles of model and observations within 4 km imply a well-mixed layer around the site.

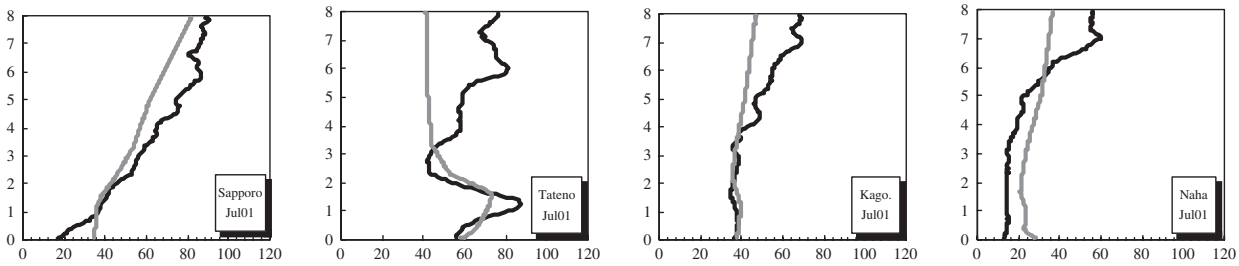

Fig. 4. Observed and modeled O_3 vertical profiles at 4 stations in Japan for July 2001; *x*-axis, O_3 concentration (ppbv); *y*-axis, altitude (km); black solid line denotes observation, from averaging over available profiles in July for each site, gray solid line means corresponding prediction. Left to right: Sapporo, Tetano, Kagoshima, and Naha.

Naha, situated in Okinawa islands south–southwest of Kagoshima, is often exposed to maritime circulations. Therefore it is not surprising to have a relatively low O_3 concentration level. Although the model overpredicts twice as much as the surface concentration, it nevertheless displays a similar constant vertical profile even up to around 5.5 km. Clearly, the vertical mixing is strong, which is typical of maritime boundary meteorology; the model is obviously capable of reproducing it.

According to Han et al. (2007), modeled O_3 profiles exhibit the widest standard deviation with respect to the ensemble averages in the July 2001 case. Our model profiles stay well within the standard deviation and closer to the ozonesondes than the ensemble means do.

4.4. Spatial distribution of O_3 and relevant species concentrations

Fig. 5 shows the spatial patterns of monthly mean ground-level O_3 generated by models in Carmichael et al. (2008) as well as by our model (last plot without ID number), for July 2001. There are a few points to note.

(1) Like all the other models, our model reproduces high O_3 over Tibet where terrain elevation is typically 4–5 km. It also displays a generally higher concentration in mid-latitude across northern China and Japan Sea. The green pattern over Japan Sea ranges 40–50 ppb, which reflects the O_3 overprediction with respect to ground-level observations at Sado. The discerning yellow and red pattern that ranges 50–60 ppb around Beijing also echoes the overprediction with local observations available in this study, although the very same model concentrations may have underpredicted observations from other site networks not included in this study.

(2) Our spatial plot also shows low-to-moderate concentration level in southern China and across Taiwan Strait. M-1, M-3, M-4, and M-6 display somewhat similar quality in this aspect (Carmichael et al., 2008). Southern China is one of the most economically active regions, thriving on manufacture industries and increasingly heavy onroad traffic, while Taiwan has infrastructures that a typical developed economy would have. Obviously economic development is followed eminently by air pollution due to increasing demand of fossil energy that increases emissions toward ozone concentrations. Streets' emission dataset, He et al. (2007), and Lee et al. (2002) covering the region clearly demonstrate the fact.

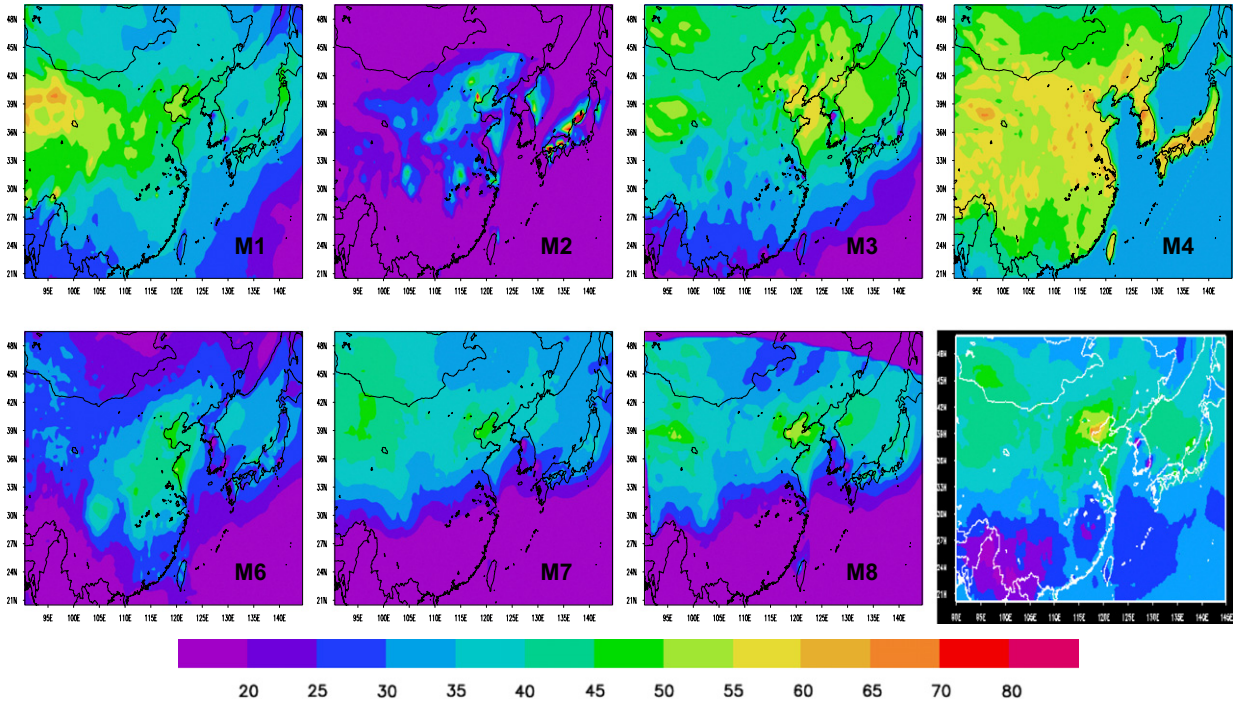

Fig. 5. Model derived monthly mean ground-level O_3 distribution (ppb) in July 2001 (the last small figure without ID number).

(3) As mentioned in Section 3 (Carmichael et al., 2008), different sets of meteorological reanalysis data are almost certain to give rise to vastly different meteorological conditions that will drastically alter the spatial distribution of air pollutants. As Carmichael et al. (2008) points out, M-7 and M-8 share exactly the same meteorology by MM5/GANAL (GANAL, Global objective ANALysis data developed by JMA), so that the overall O_3 patterns are very similar. Evidently, the extension of O_3 pattern to southern China in our model which is not captured by M-7 and M-8 is due to the choice of reanalysis data according to Carmichael et al. (2008).

Table 5
Statistics regarding daily means with respect to Taiwan and HK sites

	R	MBE	RMSE	(Pair of sample)
O_3	0.307	2.49	8.54	120

Comparison for daily means in July 2001 (unit: ppbv).

To assess the performance of our model in those regions, we further compare the model daily mean O_3 to observations from sites in Taiwan and Hong

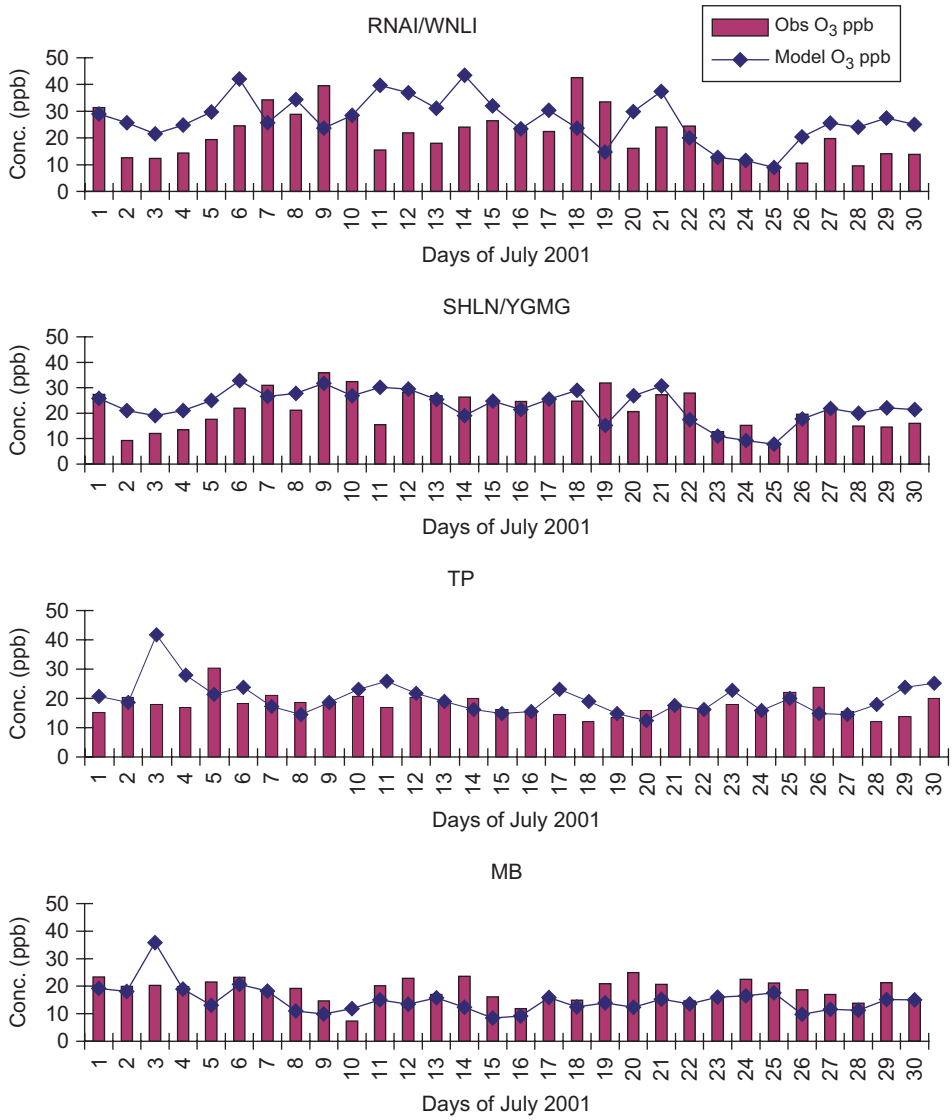

Fig. 6. Time series of modeled and observed daily mean O_3 concentrations at Taiwan (first two plots) and Hong Kong (last two plots) sites during July 2001.

Kong. The Taiwan network has been maintained by the Taiwan EPA (Taiwan Environmental Protection Administration, 2001), while Hong Kong Environmental Protection Department monitors the local air quality through its ambient monitoring network. Information can be found at http://taqm.epa.gov.tw/data/report/air90.pdf, and http://www.epd-asg.gov.hk/english/backgd/quality.php, respectively.

Two sites (SHLN/YGMG and RNAI/WNLI at north of Taiwan) in Taipei and two sites in Hong Kong (Fig. 1) were compared with the model for daily O_3. Table 5 shows the model–observation correlation, MBE and RMSE when 120 pairs of sample from these sites are used. Low correlation is reflected in Fig. 6, in which model trends are sometimes not in phase with observation trends. The positive MBE implies overprediction of these observations by the model, though the error is not too large in magnitude. The rather unsatisfactory performance is most probably due to the limitations of low grid resolution in resolving subgrid complex orography (Stoll and Porte-Agel, 2006; Hu et al., 2006). Refinement of local land use data could be another way of model improvement, since the associated albedo and moisture content can affect substantially local circulations (Lo et al., 2006). It is, however, worth to note that most of the MICS-II models underpredict the O_3 around those regions. So they may not be doing well either.

5. Conclusions

A CTM driven by MM5/NCEP reanalysis data as the meteorology, and GEOS-Chem outputs as boundary values was applied to simulate the O_3 evolution among other atmospheric chemicals for July 2001. Comparisons were made with other models in the MICS-II exercise for the same period. Statistics of both monthly and daily means show that the model skill is very good in reproducing O_3 and SO_2 with small to moderate RMSE. The model species capture the day-to-day and spatial variability of the observations. The same O_3 model concentrations that overpredict most of the EANET observations in the MICS-II study may have underpredicted ones from monitoring networks in Beijing area that is not included in this paper. Vertical O_3 profiles at 4 ozonesonde sites are well predicted in July 2001. In fact, our model performs well for statistical measurement within the 2-km surface layer. The meteorology near surface and lower troposphere is well reproduced.

The choice of reanalysis meteorological fields and different boundary conditions generated by different global models may result in diverse spatial patterns exhibited by MICS-II models and ours. Our spatial distributions of O_3 shows a high concentration patch covering Beijing, a moderate to high pattern across Korea and Japan Sea, and a low but extensive pattern enclosing southern China, Taiwan, and East Sea. Extension of the pattern to southern China coincides with the existence of pollution problems in Guangdong and Taiwan, but overprediction of O_3 over the region deserves further improvement by various factors. One of them could be the grid resolution to resolve the complex orography in or close to the ocean. Another factor can be the refinement of local land use data that changes the micro-meteorology in favor of more air pollution events, especially in the dramatically developing areas surrounding the large cities such as Beijing–Tianjin, Yangtz River Delta, and Pearl River Delta in China and Taipei in Taiwan. Further study for those areas should be conducted.

Acknowledgments

The authors acknowledge the support of the US EPA's Intercontinental Transport and Climatic Effects of Air Pollutants (ICAP) project and USEPA STAR Grant-No. R830959. The authors also thank MICS-Asia for providing the observation data and Ming-Tung Chuang for collecting Taiwan ozone monitoring data.

References

An, J., Ueda, H., Wang, Z., Matsuda, K., Kajino, M., Cheng, X., 2002. Simulations of monthly mean nitrate concentrations in precipitation over East Asia. Atmospheric Environment 36, 4159–4171.

Arndt, R.L., Carmichael, G.R., Roorda, J.M., 1998. Seasonal source–receptor relationships in Asia. Atmospheric Environment 32 (8), 1397–1406.

Byun, D.W., Ching, J.K.S., 1999. Science algorithm of the EPA Models-3 Community Multiscale Air Quality(CMAQ) Modeling System. EPA/600/R-99/030, USEPA/ORD, March 1999.

Byun, D., Schere, K.L., 2006. Review of the governing equations, computational algorithms, and other components of the Models-3 Community Multiscale Air Quality (CMAQ) modeling system. Applied Mechanics Reviews 59, 51–77.

Carmichael, G.R., Calori, G., Hayami, H., Uno, I., Cho, S.Y., Engardt, M., Kim, S., Ichikawa, Y., Ikeda, Y., Woo, J., Ueda, H., Amann, M., 2002. The MICS-Asia study: model intercomparison of long-range transport and sulfur deposition in East Asia. Atmospheric Environment 36, 175–199.

Carmichael, G.R., Tang, Y., Kurata, G., Uno, I., Streets, D., Woo, J.-H., Huang, H., Yienger, J., Lefer, B., Shetter, R., Blake, D., Atlas, E., Fried, A., Apel, E., Eisele, F., Cantrell, C., Avery, M., Barrick, J., Sachse, G., Brune, W., Sandholm, S., Kondo, Y., Singh, H., Tablot, R., Bandy, A., Thorton, D., Clarke, A., Heikes, B., 2003. Regional-scale chemical transport modeling in support of the analysis of observations obtained during the TRACE-P experiment. Journal of Geophysical Research 108 (D21), 8823.

Carmichael, G.R., Sakurai, T., Streets, D., Hozumi, Y., Ueda, H., Park, S.U., Fung, C., Han, Z., Kajino, M., Engardt, M., Bennet, C., Hayami, H., Sartelet, K., Holloway, T., Wang, Z., Kannari, A., Fu, J., Matsuda, K., Thongboonchoo, N., Amann, M., 2008. MICS-Asia II: The model intercomparison study for Asia phase II methodology and overview of findings. Atmospheric Environment 42, 3468–3490.

Carolina Environmental Programs, 2003. Sparse Matrix Operator Kernel Emission (SMOKE) Modeling System. University of Carolina, Carolina Environmental Programs, Research Triangle Park, NC.

Collela, P., Woodward, P.R., 1984. The piecewise parabolic-method (PPM) for gas dynamical simulations. Journal of Computational Physics 54, 174–201.

Chang, L., Park, S., 2004. Direct radiative forcing due to anthropogenic aerosols in East Asia during April 2001. Atmospheric Environment 38, 4467–4482.

Han, Z., Ueda, H., Matsuda, K., 2005. Model study of the impact of biogenic emission on regional ozone and the effectiveness of emission reduction scenarios over eastern China. Tellus 57B, 12–27.

Han, Z., Ueda, H., Sakurai, T., 2006a. Model study on acidifying wet deposition in East Asia during wintertime. Atmospheric Environment 40, 2360–2373.

Han, et al., 2008. MICS-Asia II: Model intercomparison and evaluation of ozone and relevant species. Atmospheric Environment 42, 3491–3509.

Hayami, H., Ichikawa, Y., 2001. Sensitivity of long-range transport of sulfur compounds to vertical distribution of sources. Water, Air, and Soil Pollution 130, 283–288.

He, Y., Uno, I., Wang, Z., Ohara, T., Sugimoto, N., Shimizu, A., Richter, A., Burrows, J., 2007. Variations of the increasing trend of tropospheric NO_2 over central east China during the past decade. Atmospheric Environment.

Heald, C.L., Jacob, D.J., Fiore, A.M., Emmons, L., Gille, J.C., Sachse, G.W., Browell, E.V., Avery, M.A., Vay, S.A., Crawford, J.H., Westberg, D.J., Blake, D.R., Singh, H.B., Sandholm, S.T., Talbot, R.W., Fuelberg, H.E., 2003. Asian outflow and transpacific transport of carbon monoxide and ozone pollution: an integrated satellite, aircraft and model perspective. Journal of Geophysical Research 108 (D24), 4804.

Holloway, T., Levy II, H., Carmichael, G.R., 2002. Transfer of reactive nitrogen in Asia: development and evaluation of a source–receptor model. Atmospheric Environment 36 (26), 4251–4264.

Hu, Y., Odman, M.T., Russell, A.G., 2006. Mass conservation in the community multiscale air quality model. Atmospheric Environment 40, 1199–1204.

Jacob, D.J., Prather, M.J., Rasch, P.J., Shia, R., Balkanski, Y.J., Beagley, S.R., Bergmann, D.J., Blackshear, W.T., Brown, M., Chiba, M., Chipperfield, M.P., de Grandpre, J., Dignon, J.E., Feichter, J., Genthon, C., Grose, W.L., Kasibhatla, P.S., Kohler, I., Kritz, M.A., Law, K., Penner, J.E., Ramonet, M., Reeves, C.E., Rotman, D.A., Stockwell, D.Z., Van Velthoven, P.F.J., Verver, G., Wild, O., Yang, H., Zimmermann, P., 1997. Evaluation and intercomparison of global atmospheric transport models using ^{222}Rn and other short-lived tracers. Journal of Geophysical Research 102 (D5), 5953–5970.

Kajino, M., Ueda, H., Satsumabayashi, H., An, J., 2004. Impacts of the eruption of Miyakejima volcano on air quality over far east Asia. Journal of Geophysical Research 109 (D21204).

Kanakidou, M., Dentener, F.J., Brasseur, G.P., Berntsen, T.K., Collins, W.J., Hauglustaine, D.A., Houweling, S., Isaksen, I.S.A., Krol, M., Lawrence, M.G., Muller, J.-F., Poisson, N., Roelofs, G.J., Wang, Y., Wauben, W.M.F., 1999. 3-D global simulations of tropospheric CO distributions—results of the GIM/IGAC intercomparison 1997 exercise. Chemosphere 1, 263–282.

Kiley, C.M., Fuelberg, H.E., Palmer, P.I., Allen, D.J., Carmichael, G.R., Jacob, D.J., Mari, C., Pierce, R.B., Pickering, K.E., Tang, Y., Wild, O., Fairlie, T.D., Logan, J.A., Sachse, G.W., Shaack, T.K., Streets, D.G., 2003. An intercomparison and evaluation of aircraft-derived and simulated CO from seven chemical transport models during the TRACE-P experiment. Journal of Geophysical Research 108 (D21), 8819.

Lee, Y.C., Calori, G., Hills, P., Carmichael, G.R., 2002. Ozone episodes in urban Hong Kong 1994–1999. Atmospheric Environment 36 (12), 1957–1968.

Lo, J.C.F., Lau, A.K.H., Fung, J.C.H., Chen, F., 2006. Investigation of enhanced cross-city transport and trapping of air pollutants by coastal and urban land–sea breeze circulations. Journal of Geophysical Research 111, D14104.

National Research Council (NRC), 1991. Rethinking the Ozone Problem in Urban and Regional Pollution. National Academy Press, Washington, DC, 489pp.

Olson, J., Prather, M., Berntsen, T., Carmichael, G., Chatfield, R., Connell, P., Derwent, R., Horowitz, L., Jin, S., Kanakidou, M., Kasibhatla, P., Kotamarthi, R., Kuhn, M., Law, K., Penner, J., Perliski, L., Sillman, S., Stordal, F., Thompson, A., Wild, O., 1997. Results from the intergovernmental panel on climatic change photochemical model intercomparison (PhotoComp). Journal of Geophysical Research 102 (D5), 5979–5991.

Phadnis, M.J., Carmichael, G.R., Ichikawa, Y., Hayami, H., 1998. Evaluation of long-range transport models for acidic deposition in East Asia. Journal of Applied Meteorology 37, 1127–1142.

Stoll, R., Porte-Agel, F., 2006. Dynamic subgrid-scale models for momentum and scalar fluxes in large-eddy simulations of neutrally stratified atmospheric boundary layers over heterogeneous terrain. Water Resources Research 42 (1).

Streets, D.G., Bond, T.C., Carmichael, G.R., Fernandes, S.D., Fu, Q., He, D., Klimont, Z., Nelson, S.M., Tsai, N.Y., Wang, M.Q., Woo, J.-H., Yarber, K.F., 2003. An inventory of gaseous and primary aerosol emissions in Asia in the year 2000. Journal of Geophysical Research 108 (D21), 8809.

Streets, D.G., Fu, J.S., Jang, C.J., Hao, J., He, K., Tang, X., Zhang, Y., Wang, Z., Li, Z., Zhang, Q., Wang, L., Wang, B., Yu, C., 2007. Air quality during the 2008 Beijing olympic games. Atmospheric Environment 41, 480–492.

Taiwan Environmental Protection Administration, 2001. Air Quality Annual Report, Taiwan area in 2001. 221pp (in Chinese).

Ueda, H., Takemoto, T., Kim, Y.P., Sha, W., 2000. Behaviors of volatile inorganic components in urban aerosols. Atmospheric Environment 34, 353–361.

Walcek, C.J., Taylor, G.R., 1986. A theoretical method for computing vertical distributions of acidity and sulfate production within cumulus clouds. Journal of Atmospheric Sciences 43, 339–355.

Wang, Z., Akimoto, H., Uno, I., 2002. Neutralization of soil aerosol and its impact on the distribution of acid rain over east Asia: observations and model results. Journal of Geophysical Research 107 (D19), 4389.

Wesely, M.L., 1989. Parameterization of surface resistances to gaseous dry deposition in regional-scale numerical models. Atmospheric Environment 23, 1293–1304.